Chapter 14
Nanocellulose as Polymer Composite Reinforcement Material

Benu George, Nidhi Lal, and T. V. Suchithra

Contents

14.1 Introduction

There is an increasing demand for bio-based materials which are degradable and free from causing environment crisis caused by non-renewable and nondegradable materials. Thus researchers are inclined to develop materials that can be durable and cost-effective to reduce.

the destruction caused by industrial and technological development (Abdul Khalil et al. 2016). Cellulose is a perfect candidate for a biomaterial which is even abundantly available (De Moura et al. 2011). Through plant photosynthesis, cellulosic fibers are plant derived embedded in hemicellulose and lignin (Karimi

B. George · N. Lal · T. V. Suchithra (✉)
School of Biotechnology, National Institute of Technology, Calicut, Kerala, India
e-mail: drsuchithratv@nitc.ac.in

R. Prasad (ed.), *Plant Nanobionics*, Nanotechnology in the Life Sciences,
https://doi.org/10.1007/978-3-030-16379-2_14

et al. 2014). The top-down approach is used to extract cellulose and used to reinforce polymers for multifunctional architectures (Karimi et al. 2014). They comprise of cellulosic material within one nanometer range whereas the elementary fibrils are made up of cellulose molecule is about 5 nm (Minelli et al. 2010). Upon the method of preparation nanocellulose is bifurcated into nanofibrillated cellulose (NFC) and cellulose nanocrystals (CNC) (Thiripura Sundari and Ramesh 2012). After complete dissolution of the noncrystalline fractions by chemical hydrolysis, nanocellulose crystal can be extracted from cellulose fibers whereas nano-fibrillated cellulose produced by high pressure and shearing forces of mechanical fibrillation after pre-treatment (Besbes et al. 2011). Polymeric reinforcement property of NFC and CNC as polymeric reinforcement have been extensively introduced, but when compared between both CNF proved to be more desirable due to its load-bearing constituents, greater ability to improve toughness, strength, and stiffness between matrix (Srithep et al. 2013). CNS's have about 65–95% crystalline nature and higher modulus of 138–150 GPa than NFC 70 GPa, theoretical such value of modulus represents a perfect crystal (Lu and Hsieh 2010). NFC provides highly flexible fibrils with better reinforcement property as they easily interconnect and form rigid web-like fibrils networks (Silvério et al. 2013). Irrespective of its advantages, NFCs have some disadvantages in polymer matrix during extrusion compounding, mostly because of its network structure and high aspect ratio. It tends to get coaggregated or actively entangles the long nanofibrils via strong hydrogen bonding (Lee et al. 2011). Furthermore, NFC consist of disordered amorphous segments which pose a threat to the mechanical properties as a filler and even composites by lowering the density (Zimmermann et al. 2010).

Hence, the chemically derived CNC from various cellulosic sources (Fig. 14.1) is of particular interest as it is a superior reinforcement agent in a polymer (Abdul Khalil et al. 2016; Rebouillat and Pla 2013; Jonoobi et al. 2009). Mainly, the wide availability of cellulose sources, potential mitigation of other inorganic reinforcing agent and the biodegradability of cellulose materials feature make it advantageous over other available reinforcement material.

As CNC have been gaining widespread attention as a versatile material with applications like structural reinforcement and as a biomedical material for tissue engineering, drug delivery, tissue repair, as carrier material for immobilization of enzymes or other proteins and as tissue substitutes. The material exhibits an extraordinary physical and chemical properties that make it biocompatible and relatively less toxic. Being of non- petroleum origin, it is also very sustainable as well as renewable. Naturally, occurring cellulose has the primary function of conferring structural integrity, and therefore mechanical strength to plants. It is therefore unsurprising that this property of nanocellulose is harnessed in reinforcing other materials. The underlying reason for this strength is the presence of surface hydroxyl groups, which cause them to self- associate, which in turn also affects their ability to be uniformly dispersed in a polymer matrix (Dufresne 2013).

Most naturally occurring polysaccharides contain both crystalline and amorphous material, from which it is possible to degrade the amorphous regions alone under controlled conditions, leaving the crystalline part undamaged. Nanocellulose obtained through different forms is product of cellulose sourced through plant, ani-

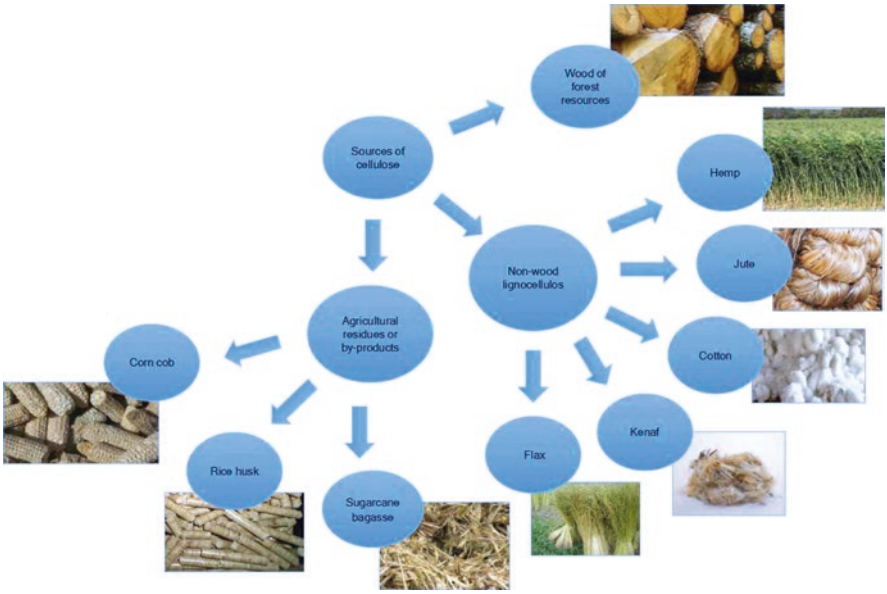

Fig. 14.1 Various potential natural sources of cellulose

mal and bacteria. Thus they are simplified by classifying them in three class (a) cellulose nanocrystals (CNC), also referred as nanocrystalline cellulose, cellulose (nano) whiskers, rod-like cellulose microcrystals; (b) cellulose nanofibrils (CNF), also known as nanofibrillated cellulose (NFC), microfibrillated cellulose (MFC), cellulose nanofibers; and (c) bacterial cellulose (BC), re-framed as microbial cellulose. CNCs and CNFs are obtained from most plant materials, with some common sources being wood, sugarcane, hemp, sugar beet, potato tuber, algae, and cotton. CNCs are primarily produced by acid hydrolysis and heat controlled techniques, while CNFs are produced from cellulosic fibers by three methods: mechanical treatments which include homogenization, grinding, and milling, chemical treatments which include TEMPO oxidation, and combinations of chemical and mechanical treatment methods (Abitbol et al. 2016).

The third type of nanocellulose is bacterial (BC) or microbial cellulose in origin. While the first two classes use a chemically or physically induced deconstructing strategy, bacterial cellulose is synthesized and assembled into its characteristic structure by the organism. Cellulose of microbial origin contains less or no impurities like hemicelluloses, lignin, and pectin and hence does not require intensive purification (Lin and Dufresne 2014). Nevertheless, its production is somewhat limited on a commercial scale compared to CNC and CNF, due to high costs and low yield (Lin and Dufresne 2014). Several novel techniques of nanocellulose extraction have also come into existence during recent times, such as enzyme mediated production, mechanical separation processes like ceramic membrane filtration, sonochemical-assisted hydrolysis and combined mechanical shearing, enzymatic and acid hydrolysis extraction (Lin et al. 2012). The recent focus has been on optimizing the extraction process to become more energy efficient, and as a result, the

fibers are first treated physically, chemically, or enzymatically before homogenization (Klemm et al. 2011). Having exceptional physical and chemical properties, nanocellulose could potentially revolutionalize many spheres of science, most importantly biomedical engineering.

This entry focuses on physical properties of nanocellulose which places these materials as a perfect candidate for reinforcement in polymers and its production stages. The present literature also highlights the possible modification which will enhance the properties of nanocrystals for strengthening.

14.1.1 Cellulose Nanocrystals Plant Derived

A plant cell consists of an extra cytoplasmic boundary, a non-homogenous membrane of a complex, layered structure with thin peripheral primary wall and secondary wall. The secondary wall is made up of three distinct layers, out of which the middle layer consists of cellulose fibers which maintain the shape and rigidness of the plant cell (Abdul Khalil et al. 2014). Lignocellulosic natural fibers encompass the middle layer which comprises lignin and hemicelluloses (Kalia et al. 2011). Besides it consist of some other non-structural components like waxes, pectin, inorganic salts and nitrogenous salts also existed in cellulose fibers (Majeed et al. 2013). The cellulose fibers, is surrounded by polysaccharides and glycoproteins like lignin, hemicellulose and pectin (Abdul Khalil et al. 2014). It is an assembly long-chain cellulose microfibrils that form bricks to the middle layer (Kalia et al. 2011). An estimate of 30-100 individual cellulose molecules chain together and form the elementary fibrils at nano-scale of cellulose fibers (Lavoine et al. 2012). The primary units are a repetitive linear syndiotactic polysaccharide, consist of D-glucose and β-D hydroglucopyranose units linked by β-(1 → 4)-glycosidic bonds (Brinchi et al. 2013; Jiang and Hsieh 2013). The structural units are held together by inter and intra hydrogen bonding thus the assembly is known as microfibrils or nano-sized fibrils (Abdul Khalil et al. 2016).

The interchain bonds at equatorial region due to the presence of three hydroxyl (OH) group in each glucopyranose unit of cellulose chains (Kalia et al. 2011). These bonds can be stabilized by specific chemical process that results to highly ordered crystalline rods (Panaitescu et al. 2013; Alemdar and Sain 2008). But due to the absence of hydroxyl group in particular region, cellulose fibre form amorphous cellulose segments which are further apart with lower density in the crystalline structure (Dalmas et al. 2006). Nevertheless, through active acidic treatment, the amorphous region can be hydrolyzed and restructure it to a highly crystalline residue (Floros et al. 2012). Depending on the nature of the plant source, purification, pre-treatment and acid hydrolysis the rod-like crystalline cellulose obtained after acid treatment are known as cellulose nanocrystal of diameter range between 2 and 20 nm its lengths vary by 100 nm (Floros et al. 2012; Siqueira et al. 2010).

14.2 Distinguishable Properties of CNCs for Reinforcement Material

Factors like origin, soil characteristics, climate and age of the plant affect the structural and chemical composition of raw fibers. Thus a knowledge about properties to exploit CNCs to the best would provide a robust reinforcing filler for composite materials (Majeed et al. 2013). CNC has abundant hydroxyl groups, large specific surface area, high aspect ratio, high crystallinity, excellent mechanical properties and high thermal stability, making it a good choice as a reinforcing agent, as explained in Table 14.1.

Table 14.1 Properties of CNCs for reinforcing the purpose (Ng et al. 2015)

Specific characteristic	Features
Surface hydroxyl group abundance	Hydroxyl groups on surface render active site for hydrogen bonding with matrices
	High-stress resistance can be achieved since there is effective stress transfer between filler-matrix
	The interface is rigid filler – matrix which reduce diffusion of the water molecule and thermal properties
	The abundance of hydroxyl groups enable high reactive nature and versatility in chemical modification
	The density of hydroxyl group on surface progressed as untreated fiber < alkali treated fiber < bleached fiber < microfibrils < nanocrystal
Large specific surface area	It is estimated that a particular surface area of CNC is more than 100 $m^2\ g^{-1}$
	Bondability, as well as interfacial interaction with a compatible polymer, is amplified by high specific area
	The specific surface area is directly proportional to aspect ratio and a decrease in diameter of CNC
	Contact surface with compatible polymer increased due to the presence of abundant surface
	A more excellent molecular distribution could be archived with an increase in interfital interaction
High aspect ratio	It is a parameter that determines the reinforcing capacity of the nanofiller into a polymeric matrix
	Depending upon CNCs source and preparation conditions, nano element of aspect ratio 30-100 prove to be better reinforcement when compared to nanofillers of having lower aspect ratios.
	Its nano-enabled functional properties, tangling effects and percolation effects CNC of high aspect ratio are considered
	High aspect ratio facilitate an excellent interfacial interaction, even stress distribution, fillers display good flexible properties
	In comparison to nanofiberils which are rod-like particles, nanocrystals provide better material properties

(continued)

Table 14.1 (continued)

Specific characteristic	Features
High crystallinity	A high compact crystalline packing of cellulose chain is attained due to the presence of OH group of the monomer
	The crystalline structure is due to hydrogen bond thus makes it inaccessible to most traditional organic solvent and water
	High impermeable crystalline creates a convoluted path for the diffusion of the penetrable molecule in the polymer (e.g., water, gas, etc.)
	Inducing nucleating effect results in a much prominent hardening effect and could be observed in a crystalline polymer matrix
	Crystal packing enhances the degree of crystallization of polymer, increment of stiff and rigid crystalline structure of the polymer
Excellent mechanical properties	Crystalline region hydrogen bonds play a prominent role in fiber strength, stiffness, and functional strength
	A high elastic modulus a Youngs modulus is observed by reinforced material
	hydrogen bond stabilizes arrangement of cellulose chain in the material
	The mechanical properties of CNCs also depend on their cellulose type as they vary depending upon cellulose source
	Biodegradable and thermoplastic with noncompetitive mechanical properties limitations causing high strength CNCs could eliminate post-processing variation in properties
	Plant oil-based materials have relatively weak mechanical properties, however, by the introduction of CNC these proprieties can be modified easily
High thermal resistance	CNCs are cellulose chains arranged in a highly ordered manner attached by hydrogen bond stabilization thus the compact system impart thermal stability
	Hydrogen bonds in crystalline region interchain favor high-temperature resistance, preventing cellulose from melting
	Incorporation of CNCs in biopolymer (PLA, PHAs, etc.) would prove to a thermal stable reinforced composite
	Inherited by the property to hider heat flow thermal degradation of composite could be delayed

14.3 CNC Production Steps

The nanocrystals production involves various stages, the preparation method is detailed in Table 14.2, and the general procedure has been briefly mapped in Fig. 14.2. These stages are: (a) Separating the crystalline residue. (b) Dissolve the unordered part to washout; the process involves the mechanical size reduction, purification, and acid hydrolysis (Williamson 2015).

Thus, by mechanical treatment CNC is resolved into a stable suspension (Floros et al. 2012). Emphasising on conditions in each stage and its influence on reinforcing the ability of final product Table 14.2 will provide an insight.

Table 14.2 Production of CNC steps (Ng et al. 2015)

Stages	Process	Description	
First stage	Mechanical treatment	Through milled, grinding, cutting, etc. Clean fibers (crude) broken down	
		Powdered to order to obtain uniform size	
		Uniformity in size will offer more convenience in chemical treatment and improve swelling capacity in water	
		Commonly used Wiley mill/ Fritsch Pulverisette mill or grinding machine for chopping, milling and grinding Pulverisette mill or grinding machine	
		Milled fibers are then passed through 55-mesh to 60- mesh sieve	
		More excellent fibers improve contact surface area between chemicals and the active group as well as the rate of reaction	
	Wash treatment	Grounded fibers washed in distilled or deionized water	
		Thus fibers become soft and comfortable to split	
		Washing improves the efficiency of alkali treatment by removal of dirt and increasing the interaction of alkali solution and cellulose fiber	
		The external surface, i.e. fiber cell wall consist of impurities and wax substance which are removed by filtering	
		For ground fibers, before wash treatment, a pretreatment using soxhlet apparatus is favorable	
Second stage	Purification	Alkali treatment	Subjected to a robust base solution which enables to remove alkali soluble substance and expose short length crystallites
			Removes hemicellulose and other impurities covering fiber cell wall
			OH bonds disrupt by ionizing to become alkoxide
			The alkali treatment tends to form a vacancy in a structure which lead to swelling, changes in physical, dimension, morphology, structural and mechanical properties of the fiber
			Voids enable us to wash out wax, natural fats, pectin material along with hydroxyl groups Alkali treatment also ensures removal of hydrophobic obstruction for fiber to bond as well as the wetting issue with the polymer matrix
			Done by two methods alkali solution heating and alkali cooking by autoclave or digester
			Alkali solution heating process composed of mechanical stirring and exposure of high temperature ranged between 70 -90 °C
			Treatment by cooking process or alkaline retting involves a combination of high temperature and pressure
			For active degradation and removal of lignin and hemicellulose fibers treated with alkaline sulfate and acid sulfite chemicals. To boot the delignification process anthraquinone solution is used

(continued)

Table 14.2 (continued)

Stages	Process	Description	
		Bleach treatment	Following to alkali treatment, the residual lignin on fiber is removed by bleach treatment
			The operation involves boiling of fibers with the salt solution under the acidic condition (acetate buffer solution)
			Until white fibers are not archived the process is repeated many times
			White color indicates the relative amount of lignin is removed for further process
			CNC which are subjected to a higher number of bleach treatment is more thermally stable
Third stage	Libration of cellulose nanocrystal	Due to disordered amorphous with imperfect axial orientation, the thermal and mechanical properties are altered for CNC	
		Through acid hydrolysis, CNC can be enhanced for various reinforcements	
		Sulfuric acid treatment enables surface reaction and easy extraction of CNCs in a more stable colloid suspensions which are failed by HCl treatment	
		Further CNCs are subjected to centrifuge after acid treatment, as to extract the desired nano crystals	
		The pellet is subjected to wash bout 3-4 times to ensure complete removal of acid and its impurities	
		The precipitate is also filtered using Whatman 541 filter paper or glass microfiber filter	
		Final stage leads to drying to remove excess of water content in CNC since this water content can interfere during reinforcement process	
		Oven drying, freeze drying, supercritical drying, and spray-drying are the conventional drying methods adopted	

14.4 Characterization of Nanocellulose

The following methods have been widely used for the characterization of nanocellulose obtained by various chemical and physical treatments.

14.4.1 Measurement of Zeta Potential (ξ)

The potential at the electrochemical border between the diffuse layer on the surface of the particle and the stationary counter ions, also called the slip plane, is known as the zeta potential. In other words, zeta potential is the potential between the bulk fluid and the immobilized fluid layer absorbed on the particles present in the

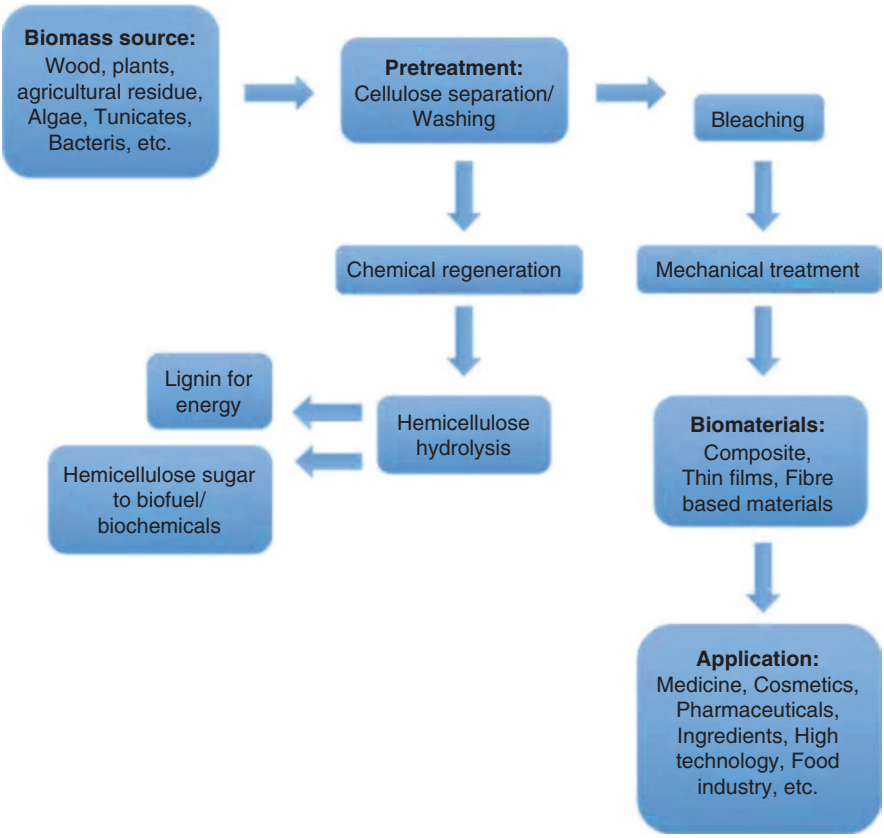

Fig. 14.2 Brief outline of CNC production steps

colloidal dispersion. It is calculated using the following formula (Uetani and Yano 2012):

$$\xi = \left(U_{\mathrm{E}}\,\eta\right) / \left(\varepsilon \mathrm{f}\left(\kappa a\right)\right)$$

Where U_{E} is the electrophoretic mobility, η is the viscosity, ε is the dielectric constant, and f(κa) is Henry's function, with the value being 1 when $\kappa a >> 1$ and 2/3 when $\kappa a << 1$. Here, κ is the inverse of Debye length and a is the major particle radius.

The electrophoretic mobility U_{E} is given by the equation:

$$U_{\mathrm{E}} = \left(\lambda \Delta \nu\right) / \left(2nE\sin\left(\theta / 2\right)\right)$$

Where, λ is the wavelength of incident light, $\Delta\nu$ is the shift in frequency, occurring due to the Doppler effect, E is the applied voltage and θ is the angle of scattering.

Cellulose nanocrystals isolated from rice straw by sulfuric acid hydrolysis, treated for 15,45 and 60 minutes have zeta potential values of −66.7 ± 0.3, −57.3 ± 2.7 and −63.8 ± 2.2 mV, respectively and cellulose nanofibrils prepared by TEMPO-mediated oxidation has a zeta potential value of −113.3 ± 1.5 mV, the negative value in the former case consistent with the presence of surface sulfate groups and in the latter case consistent with the presence of highly polar surface carboxyl groups (Jiang and Hsieh 2013).

14.4.2 X-Ray Diffraction (XRD)

X-ray diffraction can be used to study the crystallinity of the sample. With the removal of non cellulosic polysaccharides, fibers begin to align along a specific axis and show increased crystallinity. The crystallinity index is calculated using the following equation (Mwaikambo and Ansell 2002):

$$\mathrm{Ic} = \left(\mathrm{I}_{(002)} - \mathrm{I}_{(\mathrm{am})}\right) / \mathrm{I}_{(002)} \times 100$$

where Ic denotes the crystallinity index, $\mathrm{I}_{(002)}$ is the counter reading at maximum intensity at a 2θ angle of around 26°, corresponding to crystalline material and $\mathrm{I}_{(\mathrm{am})}$ is the reading at maximum intensity with a 2θ angle of around 18°, corresponding to amorphous substances. For nitrocellulose obtained from sisal fibers, the crystallinity index was found to be around 75 ± 1(Morán et al. 2008).

14.4.3 Thermal Analyses

14.4.3.1 Thermogravimetric Analysis (TGA)

TGA is used for the analysis of physical and chemical changes occurring in a substance with a change in temperature, by measuring the mass over time. TGA analysis of cellulose shows decomposition starting from 315 °C and continuing up to 400 °C (Yang et al. 2007). Cassava bagasse nanofibrils show initial decomposition at 220° due to depolymerization of starch and cellulose (Teixeira et al. 2009).

14.4.3.2 Differential Scanning Calorimetry (DSC)

DSC is an analytical technique that can reveal useful data such as glass transition temperatures, fusion temperatures, etc. The heat required to increase the temperature of a material is compared with that of reference material, and the heat

difference is measured as a function of temperature. Thermograms for nanocellulose obtained from sisal fibers show a characteristic endothermic peak from 30 °C to 140 °C due to evaporation of water and a similar mass loss of about 71% ± 3% for all the samples (Morán et al. 2008).

14.4.3.3 Fourier Transform Infrared (FTIR) Spectroscopy

FTIR is used to find the chemical structure of a compound by identification of the functional groups present in it, depending on the absorption or emission spectra obtained. The following peaks can be obtained on analysis of various samples of plant fibers: untreated plant fibers show a C=O stretch in the acetyl or uronic ester functional groups present in hemicellulose, or the ester linkage present in lignin corresponding to the peak at 1732 cm^{-1}, as well as the C=C stretch of lignin's aromatic rings corresponding to the peak at 1507 cm^{-1}, which get diminished on bleaching and acid hydrolysis, indicating the loss of hemicelluloses and lignin; C-H and C-O stretches show peaks at 2916 and 1629 cm^{-1}; O-H bending of water molecules absorbed onto cellulose show characteristic peaks at around 1647–1638 cm^{-1}, C-C ring stretch at 1151 $cm^{-1}$and C–O–C glycosidic ether linkages at 1105 cm^{-1}; all samples show C–O–C stretch of pyranose ring corresponding to bands at 1027 cm^{-1}, the glycosidic linkages between glucose units in cellulose, corresponding to bands at and 898 cm^{-1}, and the free O–H stretch from the hydroxyl groups in cellulose corresponding to the broad absorption band at around 3500–3300 cm^{-1} (Deepa et al. 2015).

14.4.4 Microscopy

The morphological and structural analysis is performed using the microscopic techniques described below:

14.4.4.1 Scanning Electron Microscopy (SEM)

This method is used specifically for the study of the morphology of nanocellulose. SEM images of raw pineapple leaf fibers show smoothly surfaced fibrils neatly stacked in bundles, which undergoes defibrillation on subjecting to a steam explosion in the presence of alkali at high temperatures due to the removal of the cementing materials, and undergoes further defibrillation on bleaching (Cherian et al. 2010).

14.4.4.2 Transmission Electron Microscopy (TEM)

Transmission electron microscopy is used for measuring dimensions of the nanocellulose particles. Although it gives good estimates of the dimensions, there is the chance that the data obtained is misleading since the conclusions are based only on a tiny sample, used in the imaging, and therefore light scattering methods may give a better overall picture. In the case of nanocellulose obtained from raw cotton linter, TEM images show agglomerated bundles of crystals with the average whisker length being 177 nm, width being 12 nm and the aspect ratio (L/D) being 19 (Morais et al. 2013).

14.4.4.3 Atomic Force Microscopy (AFM)

For cellulose fibers originating from sugarcane bagasse, treated by acid hydrolysis, both the height image (topographical image) and amplitude image (contrast image of sections of soft and hard polymer) show particles that lie in size range 70–90 nm (Mandal and Chakrabarty 2011).

14.4.5 Dynamic Light Scattering (DLS) for Measurement of Particle Size

This technique is used for statistical analysis of the size distribution of particles in a sample, by measuring the Brownian motion of suspended particles. The hydrodynamic radius (r_h), which is the radius of a spherical particle with the same viscosity or diffusion coefficient of the particle under observation, can be obtained from the Stokes-Einstein equation as follows (Fraschini et al. 2014):

For spherical particles,

$$r_h = \left(k_b T\right) / \left(6\pi\eta D_t\right)$$

Where, k_b is the Boltzmann constant (in $J.K^{-1}$), T is the absolute temperature (in K), η is the medium viscosity (in $kg.m^{-1}.s^{-1}$), D_t is the translational diffusion coefficient (in $m^2.s^{-1}$), which is obtained experimentally.

For a rod-shaped particle, D_t is calculated with the following equation:

$$D_t = \left(k_b T / \left(3\pi L\right)\right)\left(\delta - 0.5\left(\gamma^{\perp} + \gamma \|\right)\right)$$

Where, $\delta = \ln(2\ L/d)$,

$\gamma^{\perp} = -0.193 + 0.15/\delta + 8.1/\delta^2 - 18/\delta^3 + 9/\delta^4$ and

$\gamma \| = 0.807 + 0.15/\delta + 13.5/\delta^2 - 37/\delta^3 + 22/\delta^4$

Most of the particle sizes fall in the nanometric range, as can be observed in a Maxwell distribution obtained on making a plot of particle count v/s size, with the upper and lower size limits being 18.17 nm and 220 nm respectively, and the peak corresponding to 32.84 nm for nanocellulose obtained from sugarcane bagasse (Mandal and Chakrabarty 2011).

14.4.6 Birefringence Analysis

Birefringence refers to the property, where the refractive index of a substance depends on the polarization and the direction of distribution of light. This method provides an excellent way to analyze the dispersibility of nanocellulose in water, with the birefringence resulting from structural or flow anisotropy (Silvério et al. 2013). Aqueous nanocellulose suspensions have shear-induced birefringence, indicating the ability of the form of a chiral nematic liquid crystalline phase that can exist in equilibrium with isotropic phase (Fortunati et al. 2012). Casting nanocellulose suspensions can produce transparent films with a smooth surface (Deepa et al. 2015).

14.4.7 Inverse Gas Chromatography (IGC) Analysis

IGC is used for the study of surface properties of the sample, such as surface energy, surface area, free energy of adsorption, adsorption isotherm, acid-base characteristics, surface heterogeneity, monolayer capacity and permeability. The material under analysis would serve as the stationary phase, and the mobile phase contains a probe molecule. The surface properties of nanaocellulose would highly influence its ability to be used in nanocomposites, as it is a result of its chemical composition. Banana rachis nanocellulose shows dispersive surface energy (γ^{D}_{S}), Kb/Ka ratio (denotes Lewis basic character) and surface area (S_{BET}) of 43.77 mJ/m^2, 1.07 and 0.86 m^2/g respectively, while the corresponding values for sisal nanocellulose are 40.69 mJ/m^2, 1.17 and 0.82 m^2/g, those of kapok nanocellulose are 49.49 mJ/m^2, 1.00 and 0.88 m^2/g, those of pineapple leaf nanocellulose are 40.71 mJ/m^2, 1.60 and 0.82 m^2/g and those of coir nanocellulose are 48.37 mJ/m^2, 1.83 and 0.99 m^2/g (Deepa et al. 2015).

14.4.8 Rheological Characterization

Nanocellulose prepared by high-pressure homogenization of sugarcane bagasse shows a higher storage modulus (G´) than loss modulus (G”), indicating gel like properties (Li et al. 2012).

14.5 Modifications Achievable in Nanocellulose Crystals

Due to dissimilar in polarity and chemical functionality, the conjunction between hydrophobic polymers such as PLA, PE, etc. and CNCs is hindered. This cause some adverse effects as shown in Fig. 14.3 (Prateek et al. 2012; Sehaqui et al. 2011).

Thus physical/ chemical assisted surface modification of CNC is opted to improve dispersibility and compatibility of CNCs (Zhang et al. 2011). Generally, four surface modifications are preferred. Briefly, they are outlined in Table 14.3. With an aim to reduce the specific surface energy to avoid agglomeration as well as poor interfacial adhesion to the polymer matrix, these modifications are carried out (Kuo et al. 2013). Thermodynamically, due to the highly developed specific surface, nano-scale cellulose structures have enhanced thermodynamic potential. Thus attribute the reason for the instability of CNCs and form aggregation (Islam et al. 2013).

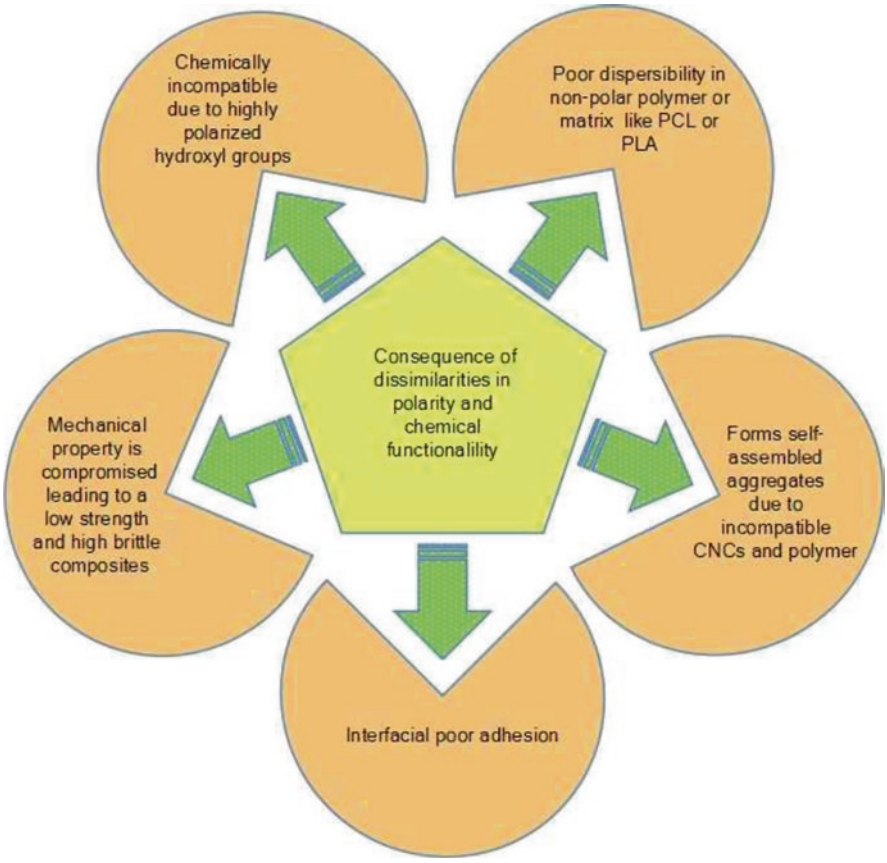

Fig. 14.3 Negative effect of dissimilarities in polarity and chemical functionality between CNC and hydrophobic polymer

Table 14.3 Modifications achievable in nanocellulose crystals (Ng et al. 2015)

Type of surface modification	Silent features
Electrostatic group introduction	The aim is to insert electrostatic group
	Such electrostatic introduction hinders the hydrogen attachment among the cellulose chain
	Most preferred treatment is carried by sulfuric acid, whereas TEMPO-mediated oxidation enhance negative charge
	Epoxypropyltrimethylammonium chloride leads to cationization of surface
	Cationization results in, (a) Aqueous suspension stability with CNC (b) Avoid thixotropic unexpected gelling (c) Retain the inherent crystal morphology
Chemical modification	Compatibilizing agent, coupling agent, acetylating agent, polymer grafting agent modification is easily possible due to surface hydroxy groups availableness
	Most favored method relays on the usage of compatibilizing agent as it induces interface bonding between contradictory phases
	The compatibilizer consist of co-polymers of the polymeric matrix and an anhydride (e.g., Maleic anhydride)
	Peroxide assisted initiator for chemical modification improve the interfacial bonding between hydrophilic CNCs and hydrophobic polymer matrix
	Alternatively another compatibilizing agent like permanganate, lignosulfonate, etc. Enhance the adhesive property
	Coupling agents (e.g., Organo functional silanes and titanate coupling agent) improve the interfacial adhesion property
	Through esterification, hydrophobic ester groups on the surface of CNC helps in covalent chemical modification
	Polymer grafting onto CNC surface could be done by, grafting-onto and grafting-from
Physical Modification	It is carried out to enhance the mechanical bonding (matrix) and properties (composite)
	The methods involved are electric discharge (corona, cold plasma), dielectric-barrier discharge, ultrasonic, irradiation, mechanochemical treatment
	To attain surface oxidation, Corona treatment is preferred
	Removal of protons and creation of unstable radicals on the surface of cellulosic material could be done by cold plasma treatment
	A better interaction between matrix-reinforcement and level of filler distribution small particle size and large specific surface area lignocelluloses are chosen

(continued)

Table 14.3 (continued)

Type of surface modification	Silent features
Bacterial Modification	Bacterial nanocellulose coat the lignocellulose surface when a cellulose-producing bacteria is grown in the presence of lignocellulose
	On the surface of natural fibers, Crystalline nanocellulose of bacteria can be seen in the form of hairy fibers
	There is an active hydrogen bonding between bacterial cellulose and the lignocellulose hydroxyl groups
	Mechanical properties in both dry and wet states, porosity, water absorbency, moldability, biodegradability, and excellent biological affinity can be easily modified

14.6 Conclusion

Nanocellulose is available abundant quantities, an inexhaustible and cheaply sourced. The production cost of CNCs is comparatively low. It can hold the account for the unused agricultural residues that are produced every year. Due to these reasons, CNC could be a better alternative than synthetic reinforcing fibers like carbon or glass. As compared to man-made engineered fillers that are harmful to environment nanocellulose are biodegradable and cause less impact to harm the environment. Such prominent characteristics of nanocellulose could be a perfect candidate as reinforcement material in bio-polymers resulting it to a superior material with apical applications for a clean future.

References

Abdul Khalil HPS, Davoudpour Y, Islam MN, Mustapha A, Sudesh K, Dungani R, Jawaid M (2014) Production and modification of nanofibrillated cellulose using various mechanical processes: a review. Carbohydr Polym 99:649–665. Elsevier BV. https://doi.org/10.1016/j.carbpol.2013.08.069

Abdul Khalil HPS, Bhat IUH, Jawaid M et al (2016) Bamboo fibre reinforced biocomposites: a review. Mater Des. https://doi.org/10.1007/s00170-016-9010-9

Abitbol T, Rivkin A, Cao Y, Nevo Y, Abraham E, Ben-Shalom T, Lapidot S, Shoseyov O (2016) Nanocellulose, a tiny fiber with huge applications. Curr Opin Biotechnol 39:76–88. Elsevier BV. https://doi.org/10.1016/j.copbio.2016.01.002

Alemdar A, Sain M (2008) Biocomposites from wheat straw nanofibers: morphology, thermal and mechanical properties. Compos Sci Technol. https://doi.org/10.1016/j.compscitech.2007.05.044

Besbes I, Vilar MR, Boufi S (2011) Nanofibrillated cellulose from Alfa, Eucalyptus and Pine fibers: preparation, characteristics and reinforcing potential. Carbohydr Polym. https://doi.org/10.1016/j.carbpol.2011.06.015

Brinchi L, Cotana F, Fortunati E, Kenny JM (2013) Production of nanocrystalline cellulose from lignocellulosic biomass: technology and applications. Carbohydr Polym

Cherian BM, Leão AL, de Souza SF et al (2010) Isolation of nanocellulose from pineapple leaf fibers by steam explosion. Carbohydr Polym. https://doi.org/10.1016/j.carbpol.2010.03.046

Dalmas F, Chazeau L, Gauthier C et al (2006) Large deformation mechanical behavior of flexible nanofiber filled polymer nanocomposites. Polymer (Guildf). https://doi.org/10.1016/j.polymer.2006.02.014

De Moura MR, Avena-Bustillos RJ, McHugh TH et al (2011) Miniaturization of cellulose fibers and effect of addition on the mechanical and barrier properties of hydroxypropyl methylcellulose films. J Food Eng. https://doi.org/10.1016/j.jfoodeng.2010.12.008

Deepa B, Abraham E, Cordeiro N et al (2015) Utilization of various lignocellulosic biomass for the production of nanocellulose: a comparative study. Cellulose. https://doi.org/10.1007/s10570-015-0554-x

Dufresne A (2013) Nanocellulose: a new ageless bionanomaterial. Mater Today. https://doi.org/10.1016/j.mattod.2013.06.004

Floros M, Hojabri L, Abraham E et al (2012) Enhancement of thermal stability, strength and extensibility of lipid-based polyurethanes with cellulose-based nanofibers. In: Polymer degradation and stability

Fortunati E, Puglia D, Monti M, Peponi L, Santulli C, Kenny JM, Torre L (2012) Extraction of cellulose nanocrystals from *Phormium tenax* Fibres. J Polym Environ 21:319–328. Springer Nature. https://doi.org/10.1007/s10924-012-0543-1

Fraschini C, Chauve G, Le Berre J-F et al (2014) Critical discussion of light scattering and microscopy techniques for CNC particle sizing. Nord Pulp Pap Res J. https://doi.org/10.3183/NPPRJ-2014-29-01-p031-040

Islam M, Alam MM, Zoccola M (2013) Review on modification of nanocellulose for application in composites. Int J Innov Res Sci Eng Technol 2:5445

Jiang F, Hsieh YL (2013) Chemically and mechanically isolated nanocellulose and their self-assembled structures. Carbohydr Polym. https://doi.org/10.1016/j.carbpol.2013.02.022

Jonoobi M, Harun J, Shakeri A et al (2009) Chemical composition, crystallinity, and thermal degradation of bleached and unbleached kenaf bast (*Hibiscus cannabinus*) pulp and nanofibers. Bioresources. https://doi.org/10.15376/biores.4.2.626-639

Kalia S, Dufresne A, Cherian BM, Kaith BS, Avérous L, Njuguna J, Nassiopoulos E (2011) Cellulose-based bio- and nanocomposites: a review. Int J Polym Sci 2011:1–35. Hindawi Limited. https://doi.org/10.1155/2011/837875

Karimi S, Tahir PM, Karimi A et al (2014) Kenaf bast cellulosic fibers hierarchy: a comprehensive approach from micro to nano. Carbohydr Polym. https://doi.org/10.1016/j.carbpol.2013.09.106

Klemm D, Kramer F, Moritz S, Lindström T, Ankerfors M, Gray D, Dorris A (2011) Nanocelluloses: a new family of nature-based materials. Angew Chem Int Ed 50:5438–5466. Wiley. https://doi.org/10.1002/anie.201001273

Kuo PY, Yan N, Sain M (2013) Influence of cellulose nanofibers on the curing behavior of epoxy/amine systems. Eur Polym J 49:3778–3787. https://doi.org/10.1016/j.eurpolymj.2013.08.022

Lavoine N, Desloges I, Dufresne A, Bras J (2012) Microfibrillated cellulose – its barrier properties and applications in cellulosic materials: a review. Carbohydr Polym

Lee SH, Teramoto Y, Endo T (2011) Cellulose nanofiber-reinforced polycaprolactone/polypropylene hybrid nanocomposite. Compos Part A Appl Sci Manuf. https://doi.org/10.1016/j.compositesa.2010.10.014

Li J, Wei X, Wang Q et al (2012) Homogeneous isolation of nanocellulose from sugarcane bagasse by high pressure homogenization. Carbohydr Polym. https://doi.org/10.1016/j.carbpol.2012.07.038

Lin N, Dufresne A (2014) Nanocellulose in biomedicine: current status and future prospect. Eur Polym J. https://doi.org/10.1016/j.eurpolymj.2014.07.025

Lin N, Huang J, Dufresne A (2012) Preparation, properties and applications of polysaccharide nanocrystals in advanced functional nanomaterials: a review. Nanoscale 4:3274. Royal Society of Chemistry (RSC). https://doi.org/10.1039/c2nr30260h

Lu P, Hsieh YL (2010) Preparation and properties of cellulose nanocrystals: rods, spheres, and network. Carbohydr Polym. https://doi.org/10.1016/j.carbpol.2010.04.073
Majeed K, Jawaid M, Hassan A, Abu Bakar A, Abdul Khalil HPS, Salema AA, Inuwa I (2013) Potential materials for food packaging from nanoclay/natural fibres filled hybrid composites. Mater Des 46:391–410. Elsevier BV. https://doi.org/10.1016/j.matdes.2012.10.044
Mandal A, Chakrabarty D (2011) Isolation of nanocellulose from waste sugarcane bagasse (SCB) and its characterization. Carbohydr Polym. https://doi.org/10.1016/j.carbpol.2011.06.030
Minelli M, Baschetti MG, Doghieri F et al (2010) Investigation of mass transport properties of microfibrillated cellulose (MFC) films. J Memb Sci. https://doi.org/10.1016/j.memsci.2010.04.030
Morais JPS, Rosa MDF, De Souza Filho MDSM et al (2013) Extraction and characterization of nanocellulose structures from raw cotton linter. Carbohydr Polym. https://doi.org/10.1016/j.carbpol.2012.08.010
Morán JI, Alvarez VA, Cyras VP, Vázquez A (2008) Extraction of cellulose and preparation of nanocellulose from sisal fibers. Cellulose. https://doi.org/10.1007/s10570-007-9145-9
Mwaikambo LY, Ansell MP (2002) Chemical modification of hemp, sisal, jute, and kapok fibers by alkalization. J Appl Polym Sci. https://doi.org/10.1002/app.10460
Ng HM, Sin LT, Tee TT et al (2015) Extraction of cellulose nanocrystals from plant sources for application as reinforcing agent in polymers. Compos Part B Eng. https://doi.org/10.1016/j.compositesb.2015.01.008
Panaitescu DM, Frone AN, Nicolae C (2013) Micro- and nano-mechanical characterization of polyamide 11 and its composites containing cellulose nanofibers. Eur Polym J. https://doi.org/10.1016/j.eurpolymj.2013.09.031
Prateek S, Ramdayal G, Kumar SU, Ashwani C (2012) Fast dissolving tablets: a new venture in drug delivery. Am J PharmTech Res 2:253–279
Rebouillat S, Pla F (2013) State of the art manufacturing and engineering of nanocellulose: a review of available data and industrial applications. J Biomater Nanobiotechnol. https://doi.org/10.4236/jbnb.2013.42022
Sehaqui H, Allais M, Zhou Q, Berglund LA (2011) Wood cellulose biocomposites with fibrous structures at micro- and nanoscale. Compos Sci Technol 71:382–387. Elsevier BV. https://doi.org/10.1016/j.compscitech.2010.12.007
Silvério HA, Flauzino Neto WP, Dantas NO, Pasquini D (2013) Extraction and characterization of cellulose nanocrystals from corncob for application as reinforcing agent in nanocomposites. Ind Crop Prod. https://doi.org/10.1016/j.indcrop.2012.10.014
Siqueira G, Bras J, Dufresne A (2010) Cellulosic bionanocomposites: a review of preparation, properties and applications. Polymers (Basel)
Srithep Y, Ellingham T, Peng J et al (2013) Melt compounding of poly (3-hydroxybutyrate-co-3-hydroxyvalerate)/ nanofibrillated cellulose nanocomposites. Polym Degrad Stab. https://doi.org/10.1016/j.polymdegradstab.2013.05.006
Teixeira E de M, Pasquini D, Curvelo AAS et al (2009) Cassava bagasse cellulose nanofibrils reinforced thermoplastic cassava starch. Carbohydr Polym. https://doi.org/10.1016/j.carbpol.2009.04.034
Thiripura Sundari M, Ramesh A (2012) Isolation and characterization of cellulose nanofibers from the aquatic weed water hyacinth – *Eichhornia crassipes*. Carbohydr Polym. https://doi.org/10.1016/j.carbpol.2011.09.076
Uetani K, Yano H (2012) Zeta potential time dependence reveals the swelling dynamics of wood cellulose nanofibrils. Langmuir 28:818–827. https://doi.org/10.1021/la203404g
Williamson M (2015) Microfibrils set to transform paper furnish. TAPPI Paper360 - March/April 2015, pp 56–58

Yang H, Yan R, Chen H et al (2007) Characteristics of hemicellulose, cellulose and lignin pyrolysis. Fuel. https://doi.org/10.1016/j.fuel.2006.12.013

Zhang W, Yang X, Li C et al (2011) Mechanochemical activation of cellulose and its thermoplastic polyvinyl alcohol ecocomposites with enhanced physicochemical properties. Carbohydr Polym. https://doi.org/10.1016/j.carbpol.2010.07.062

Zimmermann T, Bordeanu N, Strub E (2010) Properties of nanofibrillated cellulose from different raw materials and its reinforcement potential. Carbohydr Polym. https://doi.org/10.1016/j.carbpol.2009.10.045